Anomalous Hollow Electron Beams in a Storage Ring

Y. K. Wu,[1,*] J. Li,[1] and J. Wu[2]

[1]*Department of Physics, Duke University, Durham, North Carolina 27708-0319, USA*
[2]*Stanford Linear Accelerator Center, Stanford University, Stanford, California 94309, USA*

(Received 24 November 2004; published 7 April 2005)

This Letter reports the first observations of an anomalous hollow electron beam in the Duke storage ring. Created by exciting the single-bunch beam in a lattice with a negative chromaticity, the hollow beam consists of a solid core inside and a large ring outside. We report the detailed measurements of the hollow beam phenomenon, including its distinct image pattern, spectrum signature, and its evolution with time. By capturing the postinstability bursting beam, the hollow beam is a unique model system for studying the transverse instabilities, in particular, the interplay of the wakefield and the lattice nonlinearity. In addition, the hollow beam can be used as a powerful tool to study the linear and nonlinear particle dynamics in the storage ring.

DOI: 10.1103/PhysRevLett.94.134802 PACS numbers: 29.20.Dh, 29.27.Bd, 41.85.Ct

In an electron-positron circular accelerator, the charged particles circulating around the accelerator are confined in a six-dimensional phase space trap. In the transverse directions, the potential well is formed as the result of focusing fields of the magnetic optics; the longitudinal trapping is provided by the radio-frequency (rf) system which also compensates for the beam energy loss due to radiation. At the low beam current limit, the natural equilibrium beam distribution is Gaussian in all dimensions. The equilibrium beam sizes are characterized by its phase space areas, i.e., transverse and longitudinal emittances. Small emittance and high peak current are essential for achieving a high brightness in light source rings and a high luminosity in high energy physics collider rings. The development of advanced storage ring light sources and colliders aims at confining more charged particles into an increasingly smaller phase space volume.

Non-Gaussian beams can be realized by trapping charges in islands of nonlinear resonances. For example, resonance trapping has been successfully used for multiturn beam extraction of a proton synchrotron [1,2]. A theory on the beam distribution near a single nonlinear resonance has also been developed [3].

On the other hand, the observed nonresonant equilibrium beam distribution in the electron-positron storage ring, thus far, has always been a solid beam. The distribution and quality of the beam can be adversely impacted by the electromagnetic fields left behind by the beam itself. These wakefields contained by the surrounding vacuum chambers act back on the beam, which can give rise to instabilities. The beam instability can either change beam distribution or cause beam loss. For example, the longitudinal single-bunch instability, the so-called ''microwave'' instability, can increase the energy spread of the beam and lengthen the bunch without causing beam loss. The single-bunch transverse instabilities, however, can cause a fast beam blowup and, consequently, a beam loss. This blowup instability sets a limit on the maximum charge which can be confined in a single bunch. Because of their importance to the accelerator performance, the single-bunch instabilities, both transverse and longitudinal, have been the subject of many intense studies in the recent years [4–14]. Beyond a certain threshold, jittery beam phenomena have been observed in both longitudinal and transverse directions and they are described as sawtooth instability [15]. Another kind of longitudinal beam distribution beyond the threshold is described as ''binary-star'' instability [16]. While produced in simulation, this type of beam phenomenon has not been observed experimentally.

During our single-bunch threshold studies in 2003 and 2004, we observed anomalous hollow electron beams in the Duke storage ring (Fig. 1); these were first observations of single-bunch, nonsolid, transversely split beam distributions unassociated with nonlinear resonances. The term ''hollow beam'' in this work is used to describe an anomalous electron beam distribution with a transverse projection consisting of a large ring beam outside and a small core beam inside. In some cases, the solid core beam can be almost invisible due to a small amount of charge. The most critical lattice parameter to establish such a hollow beam is the slightly negative horizontal chromaticity, as small as $\xi_x = -0.07$. With a negative chromaticity, the beam initially would remain solid. When a small external excitation is applied, the beam blows up horizontally. Instead of losing charges, the blown-up beam is captured at a large transverse amplitude, forming a hollow electron beam distribution as shown in Fig. 1. All our results reported in this work were measured with a single-bunch beam at 274 MeV. The horizontal chromaticity, ξ_x, was typically between -0.4 and -0.5 while keeping the less critical vertical chromaticity close to zero. Other important parameters of the Duke storage ring are listed in Table I.

By varying lattice parameters, the size and the shape of the ring beam can be altered. Figure 1 shows two beam images with different betatron tunes; an increased coupling is seen in the lower image. The ring beam can be fit to an ellipse after the ring peaks in the radial direction are determined along the azimuth. The contours of the core

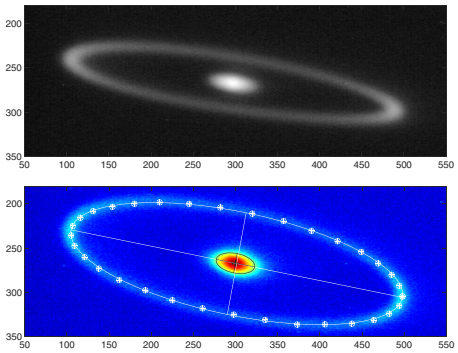

FIG. 1 (color online). Hollow beam images captured at a dipole synchrotron port with a 274 MeV electron beam for different lattice tunes. Upper plot: A raw image with a single-bunch current of $I_b = 0.58$ mA and $\nu_x = 9.1191$. Lower plot: A pseudocolor beam image with $I_b = 0.44$ mA and $\nu_x = 9.1585$. The core beam and the ring beam are fit to ellipses which are described by $\frac{(x'-x'_0)^2}{a^2} + \frac{(y'-y'_0)^2}{b^2} = 1$, where $x' = x\cos\phi - y\sin\phi$, $y' = x\sin\phi + y\cos\phi$. The ring beam ellipse is determined using local peaks in the radial direction which are indicated by small circles. The ellipse parameters are $a = 200$, $b = 58.5$, $\phi = -0.192$ (the ring beam) and $a = 23.2$, $b = 11.1$, $\phi = -0.185$ (the core beam) Beam images in Figs. 1 and 4 are measured in pixels; the size of a pixel is $14.7(\pm 0.5)$ μm.

beam can also be fit to an ellipse. Using the fit ellipses, the size of the ring and core beams can be compared; horizontally, the ring beam can be more than 10 times the rms core beam size. In Fig. 1 (lower plot), the horizontal ring beam radius, $a = 2.94 \pm 0.10$ mm which corresponds to a horizontal phase space area of 6.6 ± 0.6 mm mrad, a significant portion of the available horizontal aperture of about 40 mm mrad. Assuming a linear optical response of the imaging system, the charge in the beam can be estimated using the integrated light intensity of the image. The charge in the ring beam can be as high as 10 times the charge in the core beam.

With a hollow beam, very distinct betatron and synchrotron spectra have been observed (Fig. 2). The betatron tune spectra (upper plot) are measured using a network analyzer. The horizontal fundamental tune line (ν_x), its harmonics ($2\nu_x$, $3\nu_x$, $4\nu_x$), and their companion harmonics ($1 - 4\nu_x$, $1 - 3\nu_x$, $1 - 2\nu_x$, $1 - \nu_x$) stand out profoundly.

TABLE I. The Duke storage ring parameters.

Operation energy [GeV]	0.27–1.2
Circumference [m]	107.46
Radio frequency [MHz]	178.55
Harmonic number	64
Damping times [ms] at 274 MeV	
Horizontal (τ_x)	890
Vertical (τ_y)	826
Energy (τ_E)	399
Natural chromaticity (ξ_x, ξ_y)	-10, -9.8
Betatron tunes (ν_x, ν_y)	9.11, 4.18
Momentum compaction (α_c)	8.6×10^{-3}

In fact, these tune lines are so strong, with a signal level typically 20 to 35 dB higher than that of a solid beam, similar spectra are observed by measuring the self-excited betatron signals. In addition to the synchrotron sidebands ($f_s = 19.4$ kHz), the signals associated with the difference frequency between $4\nu_x$ and $1 - 4\nu_x$ with a $df \approx 70$ kHz also show up as sidebands to $2\nu_x$, $3\nu_x$, $4\nu_x$ and their companion harmonics—two such stronger sidebands are labeled as $5\nu_x$ and $1 - 5\nu_x$ in the plot. It is worth pointing out that the vertical betatron signal is not visible in the spectra, completely overwhelmed by horizontal tune signals. The synchrotron spectrum measured using a spectrum analyzer and a stripline receiver also shows a very distinct behavior. The lower plot of Fig. 2 shows very strong self-excited betatron sidebands, about 25 dB above the beam revolution signal. These sidebands are otherwise invisible with a solid beam. During the above spectrum measurements, the observed hollow beam images appear fuzzier that those shown in Fig. 1 due to a larger beam current.

Once created, the hollow beam evolves in cycles over the time; Fig. 3 illustrates six such evolution cycles. Because of its large size and charge, the ring beam is the focus of our data analysis. The period of the evolution cycle is about 7 to 8 min, which consists of a long semi-stationary phase (about 98% of the time) and a rapid burst phase due to instability. After each burst, the ring beam charge and size are restored to a level similar to the previous cycle; in fact, ring beam size after a burst is rather repeatable, with less than 3% of variation in six cycles.

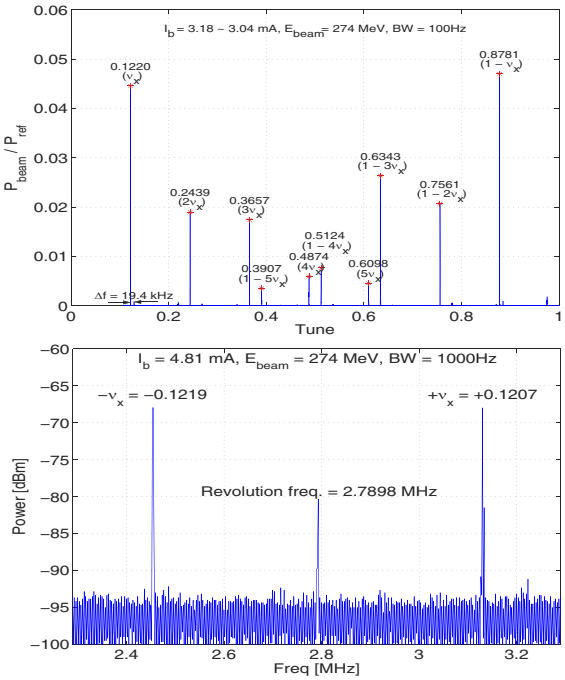

FIG. 2 (color online). Measured betatron and synchrotron spectra of a hollow beam in a 274 MeV lattice with a horizontal chromaticity $\xi_x = -0.45$. Upper plot: Measured betatron tune spectra which show the aggregated data from five consecutive measurements. Lower plot: Measured synchrotron spectrum.

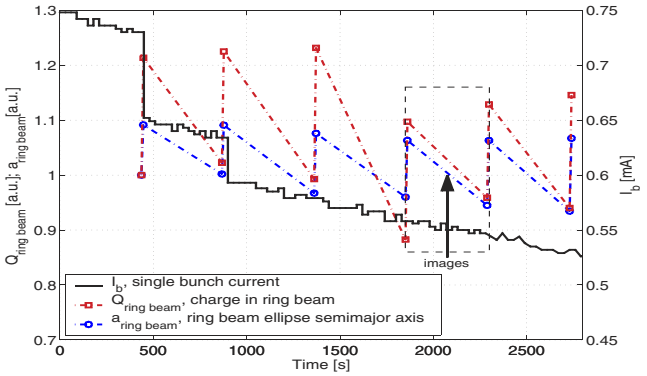

FIG. 3 (color online). Cycles of the hollow beam evolution as a function of time. The measured ring beam size and charge indicated by the squares and circles are connected by dashed lines (not measured) to improve legibility. Detailed beam images for the boxed evolution cycle are shown in Fig. 4.

These bursts can be lossless, depending on lattice and beam parameters; there is no current loss during the last four bursts and the beam lifetime is about 4.5 h with 0.58 mA of current.

Figure 4 shows selected beam images from one of the evolution cycles. Immediately after a burst between $t = 0$ and $t = 430$ s, a semistationary phase with a slow beam evolution is observed. For the ring beam, the shape of the ellipse remains mostly constant, while its size shrinks slightly by about 12%. This is accompanied by a reduction of its integrated intensity, which indicates a slow migration of charge from the ring beam to the core beam. In the meantime, the core beam gains the charge and its intensity increases by almost a factor of 2. Its shape also undergoes a slow transition to become rounder; the ellipse axis ratio, a/b, changes from a value of 2.7–2.9 between $t = 0$ and $t = 220$ s to 2.1–2.2 between $t = 270$ and $t = 430$ s.

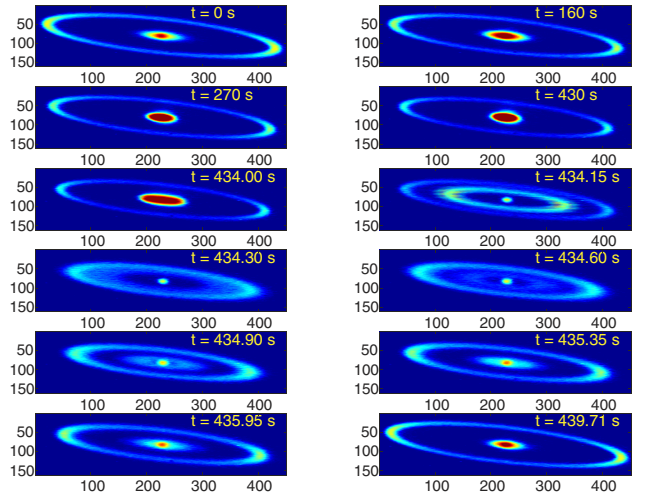

FIG. 4 (color online). A series of images captured at various of times during a cycle of beam evolution. All images are plotted using the same intensity map. A single-bunch current decreases from 0.558 mA at $t = 0$ s to 0.545 mA at $t = 440$ s.

The semistationary phase is followed by a burst phase of evolution. At $t = 434$ s, the core beam has accumulated such a large amount of charge that an instability develops inside which triggers the core beam breakup (from $t = 434$ to $t = 434.15$ s). The breakaway charge forms a new ring-shaped wave moving outward to meet the ring beam which shrinks inward (from $t = 434.15$ to $t = 434.30$ s). Part of the wave merges with the ring beam; part of the wave bounces back toward the core beam (from $t = 434.30$ to $t = 434.60$ s). Finally, both the core beam and ring beam settle down (from $t = 434.90$ to $t = 439.71$ s), which marks the beginning of a new evolution cycle.

The settling time of the ring beam can be obtained by analyzing the settling of its peak. To overcome the image noise problem, an averaging technique has been developed to compute the charge density distribution of the hollow beam by sampling it with a set of concentric ellipses of the same shape as the ring beam ellipse. This technique works well since the ring beam ellipse remains roughly unchanged during and immediately after the burst. The beam intensity is then integrated in the area sandwiched between two adjacent ellipses to yield a charge density distribution function $\rho(r, t)$, where r is the relative size of the sampling ellipse vs the ring beam ellipse just before the burst. The evolution of the charge density, $\rho(r, t)$, is shown as a water fall plot in Fig. 5. The charge wave after the core beam breakup is clearly visible. In addition, by analyzing the movement of the ring beam peak, its settling time is found to be 0.68 s, which is slightly less than one transverse damping time of the storage ring.

These kinds of hollow beams have been observed over a wide range of single-bunch currents from 5.4 mA down to 0.12 mA. This current range is below the single-bunch current threshold of about 5.5 mA limited by the transverse mode coupling instability with a zero vertical chromaticity. This threshold is estimated from the measured rate of the vertical tune reduction with increased bunch current. The fact that a solid beam can be maintained without breaking up over such a large current range strongly suggests a cer-

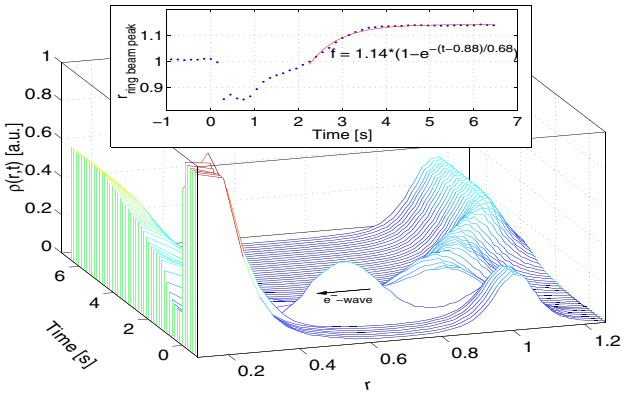

FIG. 5 (color online). Evolution of the hollow beam charge density, $\rho(r, t)$, during and after the burst. The time $t = 0$ s in this plot corresponds to the time of 434 s in Fig. 4. The inset plot shows the fit for the ring beam settling time.

tain damping mechanism against the instability. In fact, with a negative horizontal chromaticity, the beam remains solid until an external excitation is applied. The effective methods to drive apart a solid beam include introducing a horizontal orbit bump in the arc, driving a stripline kicker with an rf signal, and firing a horizontal injection kicker. After being driven apart, the ring beam and core beam can be forced to recombine by increasing the rf voltage by a factor of 3 to 5, followed by a few seconds of settling time. The formation and evolution of the hollow beam has also been monitored using a streak camera. The longitudinal profile of the beam undergoes a smooth transition during the creation of the hollow beam and periodic bursts thereafter; no longitudinal breakup of the beam has been observed. It is also worth mentioning that during the commissioning of the Duke storage ring in 1995 interesting beam images with more than one ring were observed with a multibunch beam [17] while adjusting the higher-order harmonic tuners of the rf system. At the time, we believed that these unusual beam distributions were the result of the transverse coupled bunch instability. However, because of the lack of repeatability, no follow-up studies were performed.

Our preliminary studies seem to indicate the following mechanism for the formation of the hollow beam. In a lattice with a slightly negative horizontal chromaticity, transverse instability would first increase the beam emittance; this enlarged solid beam breaks up when a small external excitation is applied. The charge flying off the beam centroid is recaptured in a new potential well at a large transverse amplitude to form a ring beam due to the nonlinear focusing of the lattice; the remaining charge in the center damps down to form the core beam. The hollow beam then undergoes repetitive cycles of a slow charge migration in the semistationary phase and a rapid charge redistribution in the burst phase in a lossless manner under certain lattice and beam conditions.

Creating a ring beam is a process of capturing the transverse instability. Consequently, the study of the hollow beam phenomenon provides unique opportunities to gain insight into the transverse instabilities and nonlinear dynamics in the storage ring. First, it remains a challenge to understand the mechanism which sustains the ring beam in the phase space; the semistationary nature of the anomalous hollow beam indicates a leaky potential well, which also awaits a theoretical explanation. Second, by capturing instability without losing current, the hollow beam phenomenon provides a powerful model system for studying transverse instabilities. In particular, this model allows the study of the delicate interplay between the wakefield and lattice nonlinearity, which has been a missing piece of the puzzle in understanding the complex mechanism of transverse instabilities. Third, because of its large dimension, the ring beam can be used as an effective tool to study particle dynamics, both linear and nonlinear. For example, by extending the ring beam to large amplitudes, the nonlinear tune shift can be measured. Finally, with a fully coupled lattice, it is conceivable that a round annular electron beam can be generated in the storage ring. The annular pattern of radiation from a circularly polarized wiggler may find its use in certain science applications.

We would like to thank the Duke free electron laser (FEL) lab engineering and operation staff for improving the storage ring stability and beam diagnostics and for assistance with the measurements. This work is supported by the medical FEL (MFEL) Grant No. F49620-001-0370 from the Air Force Office of Scientific Research and by U.S. Department of Energy Grant No. DE-FG05-91ER40665 (Y. K. W. and J. L.). This work is also supported by U.S. Department of Energy Contract No. DE-AC02-76SF00515 (J. W.).

*Electronic address: wu@fel.duke.edu

[1] R. Cappi and M. Giovannozzi, Phys. Rev. Lett. **88**, 104801 (2002).
[2] R. Cappi and M. Giovannozzi, Phys. Rev. ST Accel. Beams **7**, 024001 (2004), and references therein.
[3] A. W. Chao, Phys. Rev. ST Accel. Beams **6**, 094001 (2003).
[4] Papers and talks published in Proceedings of the Beam Instability Workshop, ESRF, Grenoble, 2000, http://www.esrf.fr/machine/conferences/BIW/PROC/proceedings.htm.
[5] U. Arp *et al.*, Phys. Rev. ST Accel. Beams **4**, 054401 (2001).
[6] J. M. Byrd *et al.*, Phys. Rev. Lett. **89**, 224801 (2002).
[7] M. Abo-Bakr *et al.*, Phys. Rev. Lett. **88**, 254801 (2002).
[8] M. Abo-Bakr *et al.*, Phys. Rev. Lett. **90**, 094801 (2003).
[9] P. Kernel, J. Revol, R. Nagaoka, and G. Besnier, in *Proceedings of the 1999 Particle Accelerator Conference (PAC), New York*, edited by A. Luccio and W. Mackay (IEEE, Piscataway, NJ, 1999), p. 1195.
[10] P. Kernel, R. Nagaoka, J. Revol, and G. Besnier, in *Proceedings of the 2000 European Particle Accelerator Conference (EPAC), Vienna* (European Physical Society, Geneva, 2000), p. 1133.
[11] J. L. Revol *et al.*, in Proceedings of the 2000 EPAC (Ref. [10]), p. 1170.
[12] K. C. Harkay *et al.*, in Proceedings of the 1999 PAC (Ref. [9]), p. 1644.
[13] K. Harkay, Z. Huang, E. Lessner, and B. Yang, in *Proceedings of the 2001 Particle Accelerator Conference, Chicago*, edited by P. Lucas and S. Webber (IEEE, Piscataway, NJ, 2001), p. 1915.
[14] Y. Minagawa *et al.*, in *Proceedings of the 2003 Particle Accelerator Conference, Portland, Oregon*, edited by Joe Chew (IEEE, Piscataway, NJ, 2003), p. 3080.
[15] P. Krejcik *et al.*, in *Proceedings of the 1993 Particle Accelerator Conference, Washington, D.C.*, edited by S. T. Corneliussen and L. Carlton (IEEE, Piscataway, NJ, 1993), p. 3240.
[16] M. D'yachkov and R. Barrtman, in *Proceedings of Fifth European Particle Accelerator Conference, Sitges (Barcelona)*, edited by S. Myers (Institute of Personal Magnetism, Miami, 1996), p. 1123.
[17] Y. Wu *et al.*, IEEE Trans. Nucl. Sci. **44**, 1753 (1997).